

Preparation of Functionalized Fe₃O₄@SiO₂ Magnetic Nanoparticles for Monoclonal Antibody Purification

HOU Xuemei¹, ZHAO Changjie¹, TIAN Yanlong², DOU Shuliang²,
ZHANG Xiang² and ZHAO Jiupeng^{1*}

1. School of Chemical Engineering and Technology, Harbin Institute of Technology,
Harbin 150001, P. R. China;

2. Center for Composite Materials, Harbin Institute of Technology, Harbin 150001, P. R. China

Abstract Magnetic Fe₃O₄@SiO₂ nanoparticles with superparamagnetic properties were prepared *via* a reverse microemulsion method at room temperature. The as-prepared samples were characterized by transmission electron microscopy(TEM), X-ray diffractometry(XRD), and vibrating sample magnetometry(VSM). The Fe₃O₄@SiO₂ nanoparticles were modified by (3-aminopropyl)triethoxysilane(APTES) and subsequently activated by glutaraldehyde(Glu). Protein A was successfully immobilized covalently onto the Glu activated Fe₃O₄@SiO₂ nanoparticles. The adsorption capacity of the nanoparticles was determined on an ultraviolet spectrophotometer(UV) and approximately up to 203 mg/g of protein A could be uniformly immobilized onto the modified Fe₃O₄@SiO₂ magnetic beads. The core-shell of the Fe₃O₄@SiO₂ magnetic beads decorated with protein A showed a good binding capacity for the chimeric anti-EGFR monoclonal antibody(anti-EGFR mAb). The purity of the anti-EGFR mAb was analyzed by virtue of HPLC. The protein A immobilized affinity beads provided a purity of about 95.4%.

Keywords Magnetic; Fe₃O₄@SiO₂; Protein A; Nanoparticle; Monoclonal antibody

1 Introduction

Magnetic nanomaterials have attracted significant attention in the past few decades due to their unique magnetic properties and potential application in the fields of biology and biomedicine^[1–5]. In particular, superparamagnetic nanoparticles have been extensively pursued for bioseparation, drug delivery, and cancer detection. Among various magnetic nanoparticles, magnetite(Fe₃O₄) has been considered as an ideal candidate for these bio-related applications because of its good biocompatibility, magnetic responsivity and low cytotoxicity^[6,7]. In 1996, iron oxide magnetic nanoparticles(MNPs) based ferumoxides(Feridex I.V.) were approved by the US Food and Drug Administration(FDA) as an imaging agent for the detection of liver lesions. Currently iron oxide MNPs are also widely used in the separation and purification of antibodies, magnetic resonance imaging(MRI) contrast enhancement, clinic diagnosis and treatment, drug delivery, and biomolecular detection^[8–10].

A considerable number of core-shell magnetic nanoparticles have been synthesized, which are commonly composed of a Fe₃O₄ magnetic core and a chemically modifiable shell, such as Au^[11], SiO₂^[12], LDH^[13], polystyrene(PS)^[14], poly(glycidyl methacrylate)(PGM)^[15], etc. Among them, SiO₂

has been considered to be one of the best materials for shell due to its advantages in magnetic property maintenance for the Fe₃O₄ core, reliable chemical stability, biocompatibility, and versatility in surface modification^[16].

Kohler and Milstein^[17] discovered monoclonal antibodies in 1975 and thus the modern era of targeted therapy for cancer began. Therapeutic antibodies have become a major strategy in clinical oncology due to their ability to specifically bind to primary and metastatic cancer cells with high affinity and create antitumor effects by complement-mediated cytotoxicity and antibody-dependent cell mediated cytotoxicity(naked antibodies). The recent clinical and commercial successes of anti-cancer antibodies, such as rituximab(Rituxan) and cetuximab(Erbitux) have created a great interest in antibody-based therapeutics for hematopoietic malignancies and solid tumors. Cetuximab is a murine-human chimeric antibody composed of the variable regions of a murine anti-EGFR antibody joined with human IgG1 heavy and light chain regions. It binds to the extracellular domain of the Epidermal Growth Factor receptor(EGFR) with a twofold greater affinity than that of its natural ligand EGF and transforming growth factor- α ^[18–20]. In addition to its role in curing colorectal carcinoma(CRC), cetuximab is approved by both FDA and the European Medicines Agency(EMA) for the treatment of locally advanced untreated

*Corresponding author. E-mail: jiupengzhao@126.com

Received June 15, 2016; accepted September 22, 2016.

Supported by the National Natural Science Foundation of China(Nos.51572058, 91216123, 51174063), the Natural Science Foundation of Heilongjiang Province, China(No.E201436), the International Science & Technology Cooperation Program of China(Nos.2013DFR10630, 2015DFE52770) and the Specialized Research Fund for the Doctoral Program of Higher Education of China(No.SRFDP 20132302110031).

© Jilin University, The Editorial Department of Chemical Research in Chinese Universities and Springer-Verlag GmbH

squamous cell carcinoma of the head and neck(SCCHN) in combination with chemoradiotherapy, which is a single agent for metastatic or recurrent disease.

Separation and purification of bio-products, such as proteins, antibodies, amino acids, polysaccharides, and vitamins are an important task of bio-processing industries. Up to now, almost 70%—80% of antibody purification is based on protein A or G affinity chromatography^[21–24]. Antibodies are produced *via* very complex processes. Before purification, there are many impurities in a sample, such as many micro-sized insoluble impurities, lipid and lipoproteins, etc., which can easily clog the chromatographic column. This may lead to issues like high back pressure, long processing time, etc. and can be a huge disadvantage in practical application^[25–27]. Compared to the column technique, the suspension technique can avoid the column clog problem^[28]. However, it is known that the packing materials in protein A or G affinity chromatographic columns are very expensive. Furthermore, protein coated resin particles are very difficult to recycle in a suspension technique, which makes it unaffordable to use. Several separation systems based on magnetic nanomaterials have been developed to avoid the drawbacks of such column-based systems, such as hierarchical core-shell micro/nanoflowers^[29] or polymer brush-modified magnetic nanoparticles^[30]. Protein A coated magnetic particles have become commercially available, which have been successfully employed in antibody purification.

Anti-EGFR mAb was purified with magnetic beads. A facile and efficient synthesis method of magnetic $\text{Fe}_3\text{O}_4@\text{SiO}_2$ nanoparticles was reported. Protein A was successfully covalently immobilized onto (3-aminopropyl)triethoxysilane (APTES) modified $\text{Fe}_3\text{O}_4@\text{SiO}_2$ MNPs with Glu. Owing to the inner magnetic core, the microspheres can be easily and rapidly separated from suspensions in an external magnetic field. A schematic diagram of the current study is illustrated in Scheme 1. The maximum adsorption of protein A on the magnetic affinity beads was found to be 203 mg/g. The magnetic core shell beads decorated with protein A showed a good binding capacity for chimeric anti-EGFR mAb. The anti-EGFR mAb was eluted from the magnetic beads with acetic acid/sodium acetate buffer solution. The purity of anti-EGFR mAb was analyzed with the aid of HPLC. The protein A immobilized affinity beads showed a purity of about 95.4%. Adsorption studies of anti-EGFR mAb

onto protein A immobilized affinity beads were also carried out in a continuous system. The protein A immobilized affinity beads may have potential application in the fields of drug delivery and the preparation of biosensors.

2 Materials and Methods

2.1 Materials

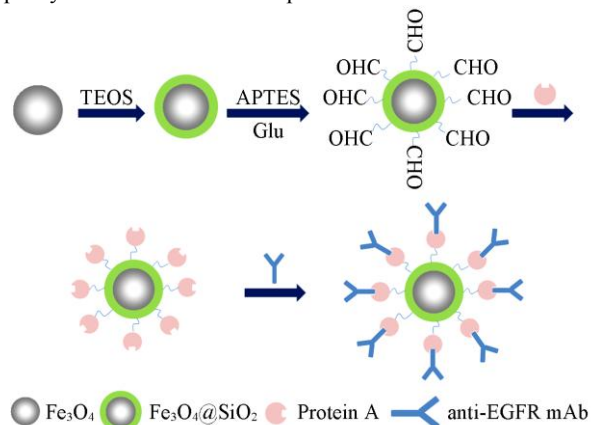
Ferric chloride hexahydrate($\text{FeCl}_3 \cdot 6\text{H}_2\text{O}$), hexane [$\text{CH}_3(\text{CH}_2)_4\text{CH}_3$], sodium chloride(NaCl), oleic acid($\text{C}_{18}\text{H}_{34}\text{O}_2$), ammonium hydroxide($\text{NH}_3 \cdot \text{H}_2\text{O}$, mass ratio 25%) and sodium hydroxide(NaOH) were purchased from Xilong Chemical Incorporated Company(Guangzhou, China). Sodium oleate ($\text{C}_{18}\text{H}_{33}\text{NaO}_2$), disodium hydrogen phosphate(Na_2HPO_4), sodium dihydrogen phosphate(NaH_2PO_4), ethanol and cyclohexane were obtained from the Fine Chemical Industry Research Institute of Tianjin City(China). Polyoxyethylene(5)nonyl-phenylether(Igepal CO-520) and 1-octadecene were obtained from Sigma Aldrich. 3-Aminopropyltriethoxysilane(APTES) and tetraethyl orthosilicate(TEOS) were purchased from the Bodi Chemical Limited Liability Company(Tianjin, China). Protein A was obtained from the Xinfeng Biological Material Limited Company. Chimeric anti-EGFR mAb was provided by Harbin Pharmaceutical Group Bioengineering Co., Ltd., China. The water used was purified through a Millipore system. All the chemicals were of analytical grade and used without further purification.

2.2 Preparation of Fe_3O_4 MNPs

Fe_3O_4 nanoparticles were prepared as described early^[31]. First, iron oleate complex was synthesized *via* the reaction of 2.7 g of $\text{FeCl}_3 \cdot 6\text{H}_2\text{O}$ with 8.875 g of sodium oleate in a mixture solution of 80 mL of ethanol, 60 mL of distilled water and 140 mL of hexane. Furthermore, 5.6 g of 1-octadecene and 1 g of iron oleate complex were dissolved in 0.16 mL of oleic acid, which was added in the vessel. The resulting mixture was heated to 320 °C at a rate of 3.3 °C/min, and kept for 30 min. The resulting solution containing the Fe_3O_4 nanocrystals was then cooled to room temperature, and excess ethanol was added to precipitate the nanocrystals. The nanocrystals were separated by means of centrifugation and washed several times with ethanol.

2.3 Synthesis of $\text{Fe}_3\text{O}_4@\text{SiO}_2$ Core-shell MNPs

A reverse microemulsion method was used to prepare $\text{Fe}_3\text{O}_4@\text{SiO}_2$ core-shell nanoparticles according to ref.[32]. Typically, 6.8 g of Igepal CO-520 was dispersed in 20 mL of cyclohexane and sonicated for 10 min. Then, 200 mL of cyclohexane containing 40 mg of Fe_3O_4 was added to the above solution with continuous stirring. Subsequently, 0.5 mL of ammonium hydroxide was added to the above mixture solution. Finally, 0.5 mL of TEOS was added in the above mixture solution *via* the equivalently fractionated drop method (adding 35 μL per 16 h). The resulted $\text{Fe}_3\text{O}_4@\text{SiO}_2$ core-shell MNPs were centrifuged and washed, and then redispersed in ethanol.



Scheme 1 Schematic illustration of the experimental overview

2.4 Amination of the Fe₃O₄@SiO₂ Core-shell MNPs

In order to functionalize the spheres with the amine functional groups, Fe₃O₄@SiO₂ core-shell nanoparticles were aminated with APTES *via* a Silylation reaction. Briefly, 0.1 g of Fe₃O₄@SiO₂ core-shell nanoparticles was mixed with 30 mL of ethanol in a three-necked flask and treated ultrasonically. Then 35 μ L of APTES was added to it. The mixture was stirred at 300 r/min for 12 h at room temperature, then was heated to 70 °C and refluxed for 1 h, and then was aged for 12 h. The nanoparticles were isolated by magnetic decantation and thoroughly washed sequentially with water and ethanol until the solution was neutralized.

2.5 Conjugation of Glu on Aminated Fe₃O₄@SiO₂ MNPs

On the surface of aminated Fe₃O₄@SiO₂ core-shell nanoparticles, there were riched amine functional groups(—NH₂), then the covalent conjugation of Glu to the MNPs was conducted. First, 10 mg of the amino-modified MNPs was mixed with 25 mL of ethanol, and then a 5% Glu solution(volume ratio or volume fraction) in 5 mL of 0.01 mol/L PBS solution(pH=7.4) was added to the mixture. The mixture was stirred at 300 r/min for 12 h at room temperature. Finally the MNPs were washed with water to remove the excess activation agent prior to protein A immobilization.

2.6 Adsorption Experiments of Protein A and Anti-EGFR mAb Binding

Protein A was covalently immobilized onto the Glu activated Fe₃O₄@SiO₂ nanoparticles, 10 mg of which was incubated with 2.5 mL of protein A solution in 0.05 mol/L PBS buffer(pH=7.4) at 25 °C in a flask with stirring at 250 r/min. After magnetic separation, the concentration of protein A in the supernatant solution was measured on a UV spectrophotometer at a detection wavelength of 276 nm. The amount of adsorbed protein A was calculated *via* the following equation:

$$Q=(c_0-c)V_s/m$$

where Q is the amount of protein A adsorbed on the affinity beads(mg/mL); c_0 and c are the concentrations of protein A in the initial solution and in the aqueous phase after adsorption, respectively; V_s is the volume of the aqueous solution(mL); and m is the mass of the affinity beads in the adsorption medium(g).

Determination of the static adsorption capacities of anti-EGFR mAb on the protein A ligands immobilized affinity beads was achieved by measuring the adsorption of anti-EGFR mAb from the aqueous solution under different experimental conditions. 10 mg of immobilized protein A-MNPs was added to a centrifuge tube containing 5 mL of anti-EGFR solution with a certain concentration and the centrifuge tube was shaken for 10 min. The affinity beads were then collected with a magnet and the supernatant was filtered through a 0.22 μ m membrane filter for HPLC analysis. The affinity beads were added

to an acetic acid/sodium acetate buffer solution(pH=3.6), and incubated with shaking to release the anti-EGFR mAb to further use.

3 Results and Discussion

3.1 Characterization of Fe₃O₄@SiO₂ MNPs

TEM images of pure Fe₃O₄ nanoparticles and Fe₃O₄@SiO₂ nanoparticles with the corresponding particle size distribution histogram are shown in Fig.1. Fe₃O₄ magnetite particles were prepared *via* a robust solvothermal reaction based on a high temperature reduction. As revealed in Fig.1(A), the obtained magnetite particles possess a uniformly spherical shape and a mean diameter of *ca.* 12 nm. Compared with the Fe₃O₄ nanoparticles, the obtained Fe₃O₄@SiO₂ nanoparticles [Fig.1(B)] exhibit a typical core-shell structure. The core-shell structure can be clearly distinguished due to the different electron penetrability between the core and shell. The magnetic cores are black spheres and the uniform silica shells are distinguished by a gray color with an average thickness of about 30 nm. The above observations demonstrate that the Fe₃O₄ nanoparticles are completely encapsulated into SiO₂ layer. Fig.1(C) shows the average size distribution of Fe₃O₄@SiO₂ nanoparticles. The result displays that the SiO₂ shells are formed homogeneously on the surfaces of Fe₃O₄ cores.

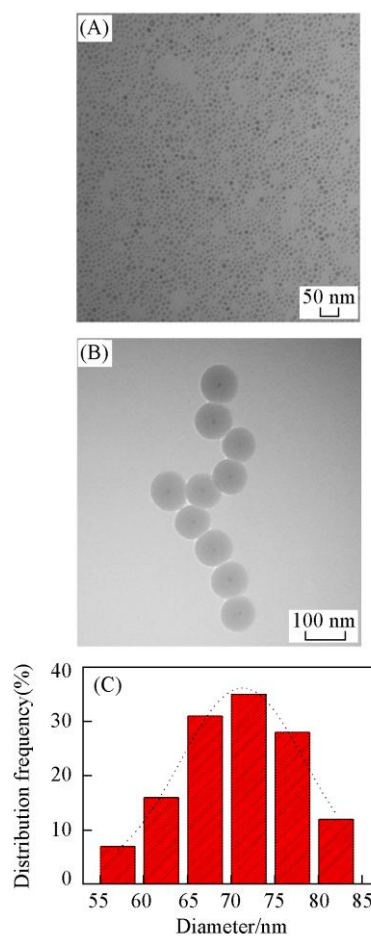


Fig.1 TEM images of Fe₃O₄(A), Fe₃O₄@SiO₂ MNPs(B) and the size distribution of Fe₃O₄@SiO₂ MNPs(C)

The phase and purity of the as-prepared samples were examined by virtue of XRD. Fig.2 shows a typical XRD pattern of the obtained Fe_3O_4 and $\text{Fe}_3\text{O}_4@\text{SiO}_2$ MNPs. As shown in curve *a*, there are six major diffraction peaks observed at 30.02° , 35.50° , 42.97° , 53.38° , 56.89° and 62.47° for the Fe_3O_4 nanocrystals, which are assigned to (220), (311), (400), (422), (511) and (440) planes of the cubic spinel structured magnetite (JCPDS No. 75-0449), respectively. No other peaks corresponding to the impurity phases can be found, indicating the high purity of the Fe_3O_4 nanoparticles. The amorphous SiO_2 exhibits no characteristic peak, and only shows a rising background at the lower angle side^[33]. After the Fe_3O_4 MNPs were coated with SiO_2 , the $\text{Fe}_3\text{O}_4@\text{SiO}_2$ MNPs show a new broad peak at 22° – 26° in curve *b*, which can be assigned to the amorphous SiO_2 . Combined with TEM results, the XRD result shows the SiO_2 has been successfully coated on the surface of Fe_3O_4 MNPs.

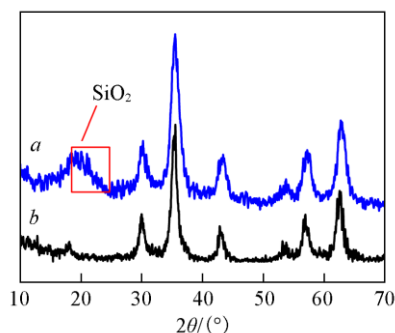


Fig.2 XRD patterns of Fe_3O_4 (*a*) and $\text{Fe}_3\text{O}_4@\text{SiO}_2$ MNPs(*b*)

In order to study their magnetic responsive behavior, the magnetic properties of the samples were measured at room temperature with VSM. Fig.3 displays the field dependence hysteresis loops (*M-H* curves) of the Fe_3O_4 and $\text{Fe}_3\text{O}_4@\text{SiO}_2$ microspheres. No reduced remanence and coercivity being zero were detected, indicating that Fe_3O_4 and $\text{Fe}_3\text{O}_4@\text{SiO}_2$ MNPs are superparamagnetic at room temperature. The saturation magnetizations of Fe_3O_4 and $\text{Fe}_3\text{O}_4@\text{SiO}_2$ microspheres were 30 and 8.5 A/m, respectively. As shown in Fig.4, when a magnet was placed on one side of the vial, the microcapsules were aggregated on the wall of the vial close to the magnet and the solution became transparent in a short period of time. Once the magnet was removed, the prepared MNPs were easily redispersed in the solution *via* gentle shaking as shown in Fig.4(A). The results demonstrate that the prepared $\text{Fe}_3\text{O}_4@\text{SiO}_2$

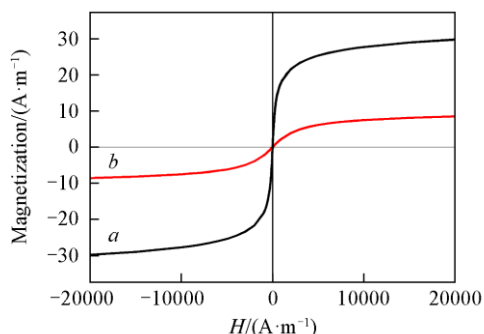


Fig.3 Magnetization curves of Fe_3O_4 (*a*) and $\text{Fe}_3\text{O}_4@\text{SiO}_2$ nanoparticles(*b*)

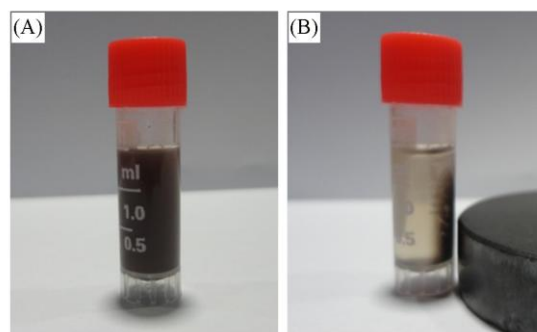


Fig.4 $\text{Fe}_3\text{O}_4@\text{SiO}_2$ MNPs dispersed in water(A) and separated by magnet(B)

MNPs exhibit excellent magnetic responsive properties, which make them possible to be applied in the field of target delivery.

3.2 Protein Loaded on $\text{Fe}_3\text{O}_4@\text{SiO}_2$ MNPs and Purification of Anti-EGFR mAb

The surface of $\text{Fe}_3\text{O}_4@\text{SiO}_2$ MNPs was modified *via* APTES-Glu method for conjugating proteins. APTES first underwent a condensation reaction on the surfaces of nanoparticles, causing the linking of APTES with the particles. Then, the Glu solution was added to the solution, and an aldehyde group reacted with the amino group of APTES *via* Schiff base formation. Another remained aldehyde group can be used for reacting with the active amino group on the protein *via* the formation of the Schiff base. As a crosslinking agent with wide applications, Glu can react more rapidly with NH_2 than NH_3^+ , which shows that Glu has its greatest potency in the neutral to alkaline pH range.

Protein A has lysine, arginine and histidine residues with pendant amine groups. Covalent immobilization of protein A onto Glu activated $\text{Fe}_3\text{O}_4@\text{SiO}_2$ MNPs was performed by the formation of Schiff base between the aldehyde group on the surface of the nanoparticles and the amino group of the protein. At the isolation point of protein A, protein A is in the best form to react with the surface aldehyde groups on the microspheres with the pendant amine groups. That is why, in this paper, protein A immobilization was carried out at a pH of 7.4 in the PBS buffer.

To determine the maximum level of the amount of immobilized protein A per unit of mass of the MNPs, a varying ratio of protein to particle was investigated as shown in Fig.5. At the

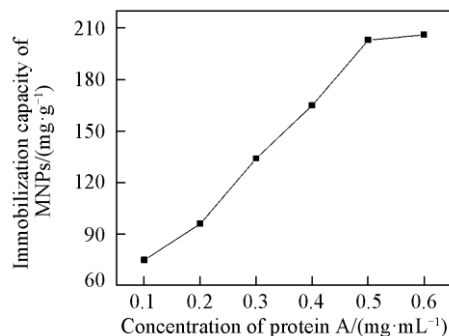


Fig.5 Loading capacity of protein A onto the surface of APTES-Glu modified $\text{Fe}_3\text{O}_4@\text{SiO}_2$ MNPs

beginning, the amount of bound protein increases as the ratio of protein to particle increases, and then increases less rapidly and the proteins loading appears to saturate as the added ratio reaches a value. The maximum amount of loaded protein A was found to be 203 mg per gram of MNPs.

Protein A has a high affinity for the Fc-part of the anti-EGFR mAb of various species, for instance human, rabbit and guinea pig, but only weak interactions occurred for bovine and mouse. Antigen-antibody can bind to mammalian cells through the interaction of the constant Fc region of immunoglobulins with Fc receptors (Fc-R) on the cell surface. The anti-EGFR mAb binding capacity was investigated at pH=7.4 and $c_0=0.4$ mg/mL. The adsorption achieved equilibrium within 10 min. The immobilization capacity was calculated to be about 112.3 mg/g.

High-pressure liquid chromatography (HPLC) is less laborious and provides more accurate and reliable quantitative results than SDS-Page for protein determination. The quantification of anti-EGFR fractions was analyzed by means of HPLC with the result indicating that about 95.4% of anti-EGFR from crude sample bound to the MNPs (Fig.6). And it is possible to elute 95.4% of pure anti-EGFR at pH=7.4.

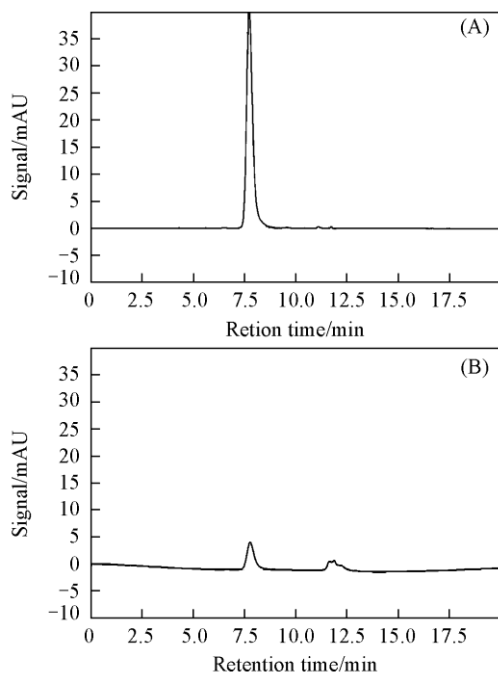


Fig.6 Chromatograms of anti-EGFR before(A) and after(B) the removal treatment with protein A immobilized on MNPs

A comparison of $\text{Fe}_3\text{O}_4@/\text{SiO}_2$ MNPs with other materials reported in the literature^[15,34] is summarized in Table 1. The purification value of the MNPs is higher than those of other samples, which suggests that the $\text{Fe}_3\text{O}_4@/\text{SiO}_2$ magnetic beads decorated with protein A show a good binding capacity for the chimeric anti-EGFR monoclonal antibody.

Table 1 Binding capacities of various particles

Sample	Purification(%)	Target
m-PGMA microspheres	61	L929 mouse fibroblasts
Immuno- $\gamma\text{-Fe}_2\text{O}_3@/\text{Au}$	88.5	Carcinoembryonic antigen
This work	95.4	Anti-EGFR monoclonal antibody

4 Conclusions

$\text{Fe}_3\text{O}_4@/\text{SiO}_2$ nanoparticles were synthesized by a reverse microemulsion method. APTES and Glu were modified on the surface of the nanoparticles. Protein A was immobilized on the APTES-Glu modified magnetic $\text{Fe}_3\text{O}_4@/\text{SiO}_2$ nanoparticles. Approximately 203 mg/g of protein A could be immobilized onto the modified $\text{Fe}_3\text{O}_4@/\text{SiO}_2$ nanoparticles. The removal of anti-EGFR in an aqueous solution by protein A immobilized on the APTES-Glu modified magnetic $\text{Fe}_3\text{O}_4@/\text{SiO}_2$ nanoparticles was studied. And the purity of anti-EGFR mAb was 95.4% which was analyzed via HPLC. This APTES-Glu surface modification can be applied to other kinds of nanoparticles for conjugating biomolecules.

References

- Lin S. Z., Chen H. H., Li Y. H., Jia R. K., *Chem. J. Chinese Universities*, **2014**, 35(12), 2529
- Cao W., Ma Y. R., Zhou W., Guo L., *Chem. Res. Chinese Universities*, **2015**, 31(4), 508
- Ovejero J. G., Bran C., Morales M. P., Vazquez M., Vi-lanova E., Kosel J., *Journal of Magnetism and Magnetic Materials*, **2015**, 389(1), 144
- Li G., Wang L., Li W., Xu Y., *Microporous and Mesoporous Materials*, **2015**, 211(15), 97
- Chen X. B., Liao D. Z., Sun Y. F., Hu X. J., Yang Y., Zhu S. J., *Chem. J. Chinese Universities*, **2005**, 26(1), 78
- Gao J., Ran X., Shi C., Cheng H., Cheng T., Su Y., *Nanoscale*, **2013**, 5(15), 7026
- Veiseh O., Gunn J. W., Zhang M., *Advanced Drug Delivery Reviews*, **2010**, 62(3), 284
- Wang W., Jing Y., He S. H., Wang J. P., Zhai J. P., *Colloids Surface B: Biointerfaces*, **2014**, 117(1), 449
- Sedlacik M., Moucka R., Kozakova Z., Kazantseva N. E., Pavlinek V., Kuritka I., Kaman O., Peer P., *Journal of Magnetism and Magnetic Materials*, **2013**, 326(1), 7
- Kaushik A., Khan R., Solanki P. R., Pandey P., Alam J., Ahmad S., Malhotra B. D., *Biosensors & Bioelectronics*, **2008**, 24(4), 676
- Cui Y., Hong C., Zhou Y., Li Y., Gao X., Zhang X., *Talanta*, **2011**, 85(3), 1246
- Hou X. M., Xu H. B., Pan L., Tian Y. L., Zhang X., *RSC Advances*, **2015**, 126(5), 103760
- Shao M. F., Ning F. Y., Zhao J. W., Wei M., Evans D. G., Duan X., *Journal of the American Chemical Society*, **2012**, 134(2), 1071
- Ji T. H., Lirtsman V. G., Avny Y., Davidov D., *Advanced Materials*, **2001**, 13(16), 1253
- Cakmak S., Gumusderelioglu M., Denizli A., *Reactive & Functional Polymers*, **2009**, 68(8), 586
- Li T., Han X., Wang Y. L., Wang F., Shi D. L., *Colloids and Surfaces A: Physicochemical and Engineering Aspects*, **2015**, 477(20), 84
- Kohler G., Milstein C., *Nature*, **1975**, 256(5517), 495
- Goldstein N. I., Prewett M., Zuklys K., Rockwell P., Mendelsohn J., *Clinical Cancer Research*, **1995**, 1(117), 1311
- Kim E. S., Khuri F. R., Herbst R. S., *Current Medical Research and Opinion*, **2001**, 13(6), 506
- Gill G. N., Kawamoto T., Cochet C., Le A., Sato J. D., Masui H., McLeod C., Mendelsohn J., *Journal of Biological Chemistry*, **1984**, 259(12), 7755

- [21] Speziale P., Pietrocola G., Rindi S., Provenzano M., Provenza G., di Poto A., Visai L., Arciola C. R., *Future Microbiology*, **2009**, 4(10), 1337
- [22] Cao Y., Tian W., Gao S. Y., Yu Y. S., Yang W. B., Bai G., *Artificial Cells Blood Substitutes & Biotechnology*, **2007**, 35(5), 467
- [23] Holschuh K., Schwammle A., *Journal of Magnetism and Magnetic Materials*, **2005**, 293(1), 345
- [24] Bailey L. J., Sheehy K. M., Hoey R. J., Schaefer Z. P., Ura M., Kosciakoff A. A., *Journal of Immunological Methods*, **2014**, 415(24), 24
- [25] Choudary B. M., Kantam M. L., Rahman A., Reddy C. V., Rao K. K., *Angewandte Chemie International Edition*, **2001**, 40(4), 763
- [26] Jain P., Sun L., Dai J., Baker G. L., Bruening M. L., *Biomacromolecules*, **2007**, 8(10), 3102
- [27] Clairbois A. S., Letourneur D., Muller D., Jozefonvicz J., *Journal of Chromatography B*, **1998**, 706(1), 55
- [28] Wang Y., Wang G., Xiao Y., Yang Y., Tang R., *ACS Applied Materials & Interfaces*, **2014**, 6(21), 19092
- [29] Xuan S. H., Wang F., Gong X. L., Kong S. K., Yu J. C., Leung K. C. F., *Chemical Communications*, **2011**, 47(9), 2514
- [30] Pan D., Zhang H., Fan T., Chen J., Duan X., *Chemical Communications*, **2011**, 47(3), 908
- [31] Park J., An K., Hwang Y., Park J. G., Noh H. J., Kim J. Y., Park J. H., Hwang N. M., Hyeon T., *Nature Materials*, **2004**, 3(12), 891
- [32] Ding H. L., Zhang Y. X., Wang S., Xu J. M., Xu S. C., Li G. H., *Chemistry of Materials*, **2012**, 24(23), 4572
- [33] Yang P. P., Quan Z. W., Hou Z. Y., Li C. X., Kang X. J., Cheng Z. Y., Lin J., *Biomaterials*, **2009**, 30(27), 4786
- [34] Lin Y., Xu G. H., We F. D., Zhang A. X., Yang J., Hu Q., *Journal of Pharmaceutical and Biomedical Analysis*, **2016**, 121(3), 135